Modification of the magnetic properties in molecular magnets based on Prussian blue analogues through adsorbed species

2006 J. Phys.: Condens. Matter 18 11243

(http://iopscience.iop.org/0953-8984/18/49/016)

INSTITUTE OF PHYSICS PUBLISHING JOURNAL OF PHYSICS: CONDENSED MATTER

J. Phys.: Condens. Matter **18** (2006) 11243–11254 doi:10.1088/0953-8984/18/49/016

Modification of the magnetic properties in molecular magnets based on Prussian blue analogues through adsorbed species

R Martinez-Garcia[1], **M Knobel**[2] **and E Reguera**[1,3,4]

[1] Institute of Materials Science and Technology, University of Havana, Cuba
[2] Instituto de Física 'Gleb Wataghin', UNICAMP, Brazil
[3] Applied Science and Advanced Technology Center, IPN, Mexico DF, Mexico

E-mail: ereguera@yahoo.com

Received 23 August 2006, in final form 19 September 2006
Published 22 November 2006
Online at stacks.iop.org/JPhysCM/18/11243

Abstract

The interaction of guest molecules (H_2O, N_2, CO_2, ethanol, methanol) with the metal ions at the pore surface in porous molecular magnets ($M_3[Fe(CN)_6]_2{\cdot}xH_2O$, M = Mn, Co, Ni, Cu) was studied by x-ray diffraction, together with Mössbauer and magnetic data. These compounds can be dehydrated at relatively low temperature, usually below 100 °C. On the removal of water a cell contraction of about 4% of the cell volume is observed. This corresponds to a shortening of the metal–metal distance and to a strengthening for the metal–metal interaction through the CN bridge groups. In these materials the outer metal (M) is always found at the pore surface and the guest–host interactions modify the electronic structure of the host solid. Such interactions and their effect on the material electronic structure were studied by Mössbauer spectroscopy for the guest molecules mentioned. The most pronounced metal–metal charge overlapping was observed for the host solid free of adsorbed species. When the guest molecules were absorbed the observed changes in the solid electronic structure followed the order $N_2 \sim CO_2 <$ ethanol $<$ methanol $<$ water. The most pronounced effect on the solid properties was observed for water, the most polar molecule within these guest species. The magnetic properties were evaluated for anhydrous and hydrated samples. The highest Curie temperature (T_C) and Curie–Weiss (θ_{CW}) constant values were found for the anhydrous solids, when the metal at the pore surface only interacts with the CN bridge groups. This corresponds to an increase in the charge delocalization among metal centres on the removal of water, an effect already detected by x-ray diffraction and Mössbauer data. Since, during the water adsorption and desorption processes, the cell symmetry is preserved, such changes for the T_C and θ_{CW} values cannot be ascribed to a variation in the linearity of the overlapping path. The observed effects are common to all the

[4] Author to whom any correspondence should be addressed.

compounds studied and not to a particular metal ion. An explanation of such behaviour for the materials studied based on a tetrahedral coordination for the metal (M) linked at the N end of the CN groups in the anhydrous phase was discarded. In the cubic structure for Prussian blue analogues a true tetrahedral coordination cannot be present.

M Supplementary data files are available from stacks.iop.org/JPhysCM/18/11243

1. Introduction

The electronic structure of solids composed of a network of open channels can be modified through adsorbed species, by means of guest–host interactions. This contribution deals with this subject: in particular, with the modification of the magnetic properties of porous molecular magnets through adsorbed species.

The study of molecular magnets is a very active and interdisciplinary research area. Prussian blue (PB) analogues, where the metal centres remain strongly linked through CN bridges, are probably the materials where the most interesting effects have been reported, e.g. high Curie temperature (T_C) magnets [1, 2], photo-induced magnetism [3], humidity-induced magnetic pole inversion [4], spin-glass behaviour [5], among others. This family of compounds offers a high flexibility to combine different metals within the same network, resulting in materials with a relatively wide diversity of physical properties [6–8]. In PB analogues with unit formula $M_3[T(CN)_6]_2{\cdot}xH_2O$, which display an open channel network, all the M atoms are sited at the pore surfaces, with the possibility of a direct interaction with the guest species within the pores. From this fact, porous molecular magnets based on PB analogues appear with unique features to explore the modification of the magnetic properties through adsorbed species, allowing one to shed light on the physical mechanisms behind the observed effects. In this study, the effect of the adsorbed species (H_2O, N_2, CO_2, ethanol, methanol) on the electronic structure of four PB analogue-based molecular magnets, in their anhydrous form, $M_3[Fe(CN)_6]_2$, where M = Mn, Co, Ni, Cu, was evaluated. The most pronounced effects were found for the adsorption and desorption of water, and from this fact the magnetic measurements were limited to this adsorbate. The magnetic measurements were complemented with x-ray diffraction (XRD), thermo-gravimetry (TG) and Mössbauer spectroscopy. Changes in the magnetic properties of molecular materials related to their crystal water is a subject that has been studied [9, 10] but, to the best of our knowledge, not from the point of view discussed here. More recently, Ohkoshi *et al* have reported [4] on the humidity-induced effects in the magnetic properties of cobalt (2+) and cobalt (2+) manganese (2+) hexacyanochromates (III). These authors discuss the observed effects according to a change in the coordination geometry for the cobalt atom. Our results for the series of hexacyanoferrates (III) studied using different adsorbates are interpreted according to the observed variation for the metal–metal charge overlapping through the CN bridges, which is more pronounced when the pore system is free of adsorbed species.

2. Experimental details

The samples studied were prepared by mixing aqueous solutions (0.01 mol l^{-1}) of ferricyanic acid (prepared *in situ* [11]) and of sulfate of the metals involved (Mn^{2+}, Co^{2+}, Ni^{2+}, Cu^{2+}). The precipitated solids were then washed several times with distilled water and dried in air until they had constant weight. All the starting reagents were analytical grade from Sigma-Aldrich.

The nature of the solids obtained as hexacyanoferrates (III) was established from IR spectra. Their stoichiometry was derived from the atomic ratio of the corresponding metals, estimated from x-ray fluorescence analyses. For all the compositions studied, M:Fe atomic ratios close to 3:2 were found. The hydration degree was calculated from thermo-gravimetric (TG) curves.

The TG curves were collected from 25 to 300 °C, under a N_2 flow (100 ml min^{-1}) using a TA instrument thermo-balance (TGA 2950 model) operated in the high-resolution mode. The IR spectra of the evolved gases, recorded *in situ*, were used to evaluate the end of the sample dehydration process and also its stability as anhydrous material. The dehydration process was also studied under vacuum at 10^{-2} Torr in order to select the most appropriate temperature and heating time to obtain anhydrous samples for adsorption experiments.

The IR spectra were recorded in Nujol mulls between KBr windows. On milling and pressing processes with KBr, ferricyanides reduce to ferrocyanides [12]. XRD powder patterns were collected with Cu Kα radiation using a Siemens D5000 diffractometer, and their preliminary evaluation was carried out using the program *Dicvol* [13]. The cell contraction on the removal of water (dehydration) was estimated from XRD powder patterns recorded in vacuum (10^{-5} Torr) for samples annealed *in situ* within the diffractometer sample holder. The samples were annealed at different temperatures, from 22 to 100 °C, for one hour and then cooled to room temperature (22 °C) to obtain the XRD pattern. These XRD patterns were recorded at the X10B beamline of the LNLS synchrotron radiation facility (Campinas, Brazil) with $\lambda = 1.796\,684$ Å, using a Ge(111) analyser crystal to optimize angular/energy resolution. Details of this experimental setup have been reported elsewhere [14]. The crystal structures were refined from XRD patterns using the Rietveld method implemented in the program *FullProf* [15]. The final refinement process was carried out using the program *GSAS* [16], which incorporates the diffuse dispersion contribution to the pattern background as one of the variables to be fitted. The magnetic data were collected at low temperature using a SQUID magnetometer (Quantum Design MPMS-XL7). The magnetic measurements were carried out for hydrated, dehydrated and rehydrated samples. The heat treatments to obtain anhydrous samples for these experiments were carried out *in situ* within the magnetometer using the sample heating option device. The Mössbauer spectra were obtained at room temperature using a constant acceleration spectrometer operated in the transmission mode with a $^{57}Co/Rh$ source. A special glass cell with windows transparent to γ-rays, which couples to an adsorption equipment to control the entrance of the species to be absorbed, was used to obtain Mössbauer spectra of anhydrous samples and with different guest species filling the material porous network. All the spectra were fitted using a pseudo-Lorentzian line shape and a least-squares minimization algorithm to obtain the values of isomer shift (δ), quadrupole splitting (Δ), linewidth (Γ) and relative area (A in %). The values of δ are reported relative to sodium nitroprusside.

As guest molecules (adsorbates), dinitrogen, carbon dioxide, ethanol, methanol and water vapour were used. Previous to the pore filling with these species the porous network was evacuated (activated) through a heating at 80 °C for 1 h in moderate vacuum (10^{-2} Torr), except for Ni which required a heating temperature of 100 °C. The adsorption process was carried out room temperature (27 °C) and normal pressure (760 Torr).

3. Results and discussion

3.1. On the nature and structure of the solids studied

All the vibrations observed in the IR spectra for the samples studied correspond to the reported absorption bands for hexacyanometallates (ν (CN), δ (FeCN), ν (FeC)) and to those from the crystal water (ν (OH), δ (HOH)) [17]. The ν (CN) vibration senses the binding of the metal

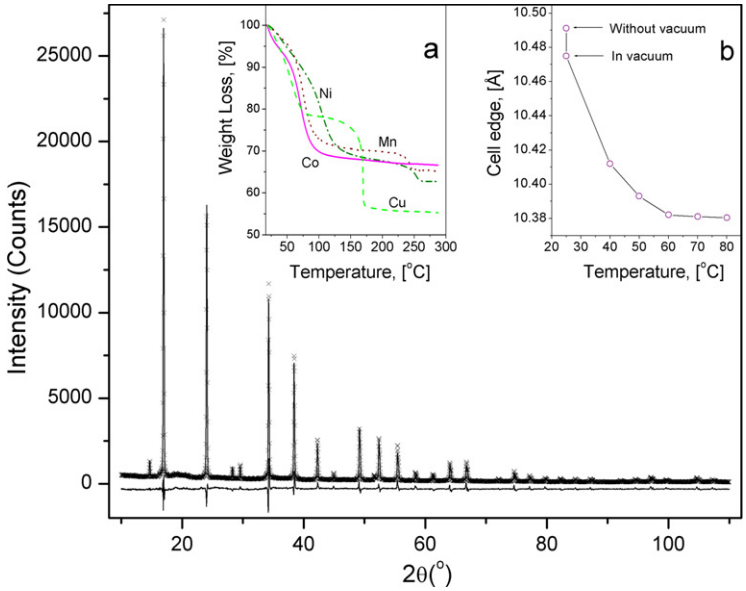

Figure 1. XRD powder pattern of $Mn_3[Fe(CN)_6]_2{\cdot}14H_2O$. This pattern corresponds to a cubic ($Fm\bar{3}m$) unit cell. Inset (a): Thermo-gravimetric curves for the materials studied. Inset (b): Cell edge variation for the manganese compound on water removal in vacuum (10^{-5} Torr).

(This figure is in colour only in the electronic version)

Table 1. Cell parameter, a in Å, at room temperature for the materials studied in their hydrated state and with their porous framework free of guest species.

Sample	Porous framework saturated of water molecules	Porous framework free of guest species
Mn_3Fe_2	10.4882(9)	10.381(1)
Co_3Fe_2	10.2794(5)	10.207(3)
Ni_3Fe_2	10.204(3)	10.073(8)
Cu_3Fe_2	10.0944(2)	10.0605(5)

ion (M) to the N end of the octahedral anionic block, $[Fe(CN)_6]^{3-}$, to form an coordination solid. Potassium ferricyanide has this vibration at 2115 cm^{-1} [12], while for the solids formed it was observed at 2167 (Mn), 2187 (Co), 2166 (Ni) and 2174 (Cu) cm^{-1}, for a frequency shift of about 50 cm^{-1} due to the coordination bond formation.

The XRD powder patterns for the as-synthesized samples (hydrates) (figure 1) correspond to the cubic cell typical of PB analogues [18]. The calculated cell parameter values (a), from these patterns, are collected in table 1. The crystal structure of this family of materials results from a 3D arrangement of octahedral anionic blocks $[Fe(CN)_6]^{3-}$ linked at their N ends by metal ions, M^{2+}. In typical PB analogues the metal centres (Fe and M atoms) have octahedral coordination, and according to the unit formula for the series studied, $M_3[Fe(CN)_6]_2{\cdot}xH_2O$, in the material framework 1/3 of the $Fe(CN)_6$ sites are vacant, creating a network of pores of about 8.5 Å in diameter that remain communicated by windows of about 4.5 Å (the interstitial free spaces). At the pore surface of the as-prepared material six M atoms are found with a mixed coordination sphere, $M(NC)_4(H_2O)_2$. The pore filling is completed with zeolitic waters linked to the coordinated ones through hydrogen-

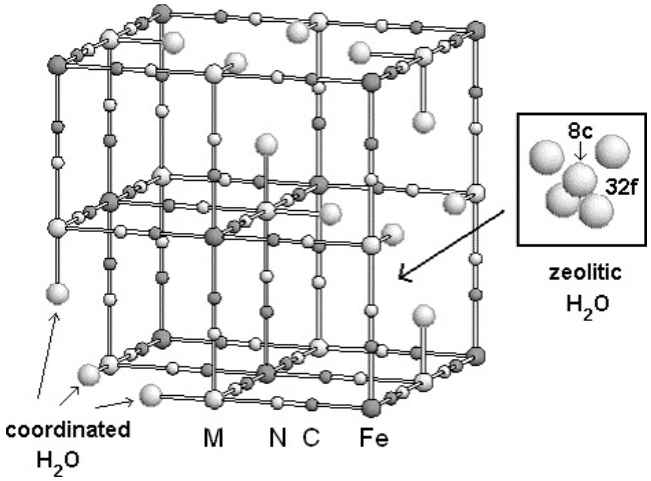

Figure 2. Unit cell for the studied family of Prussian blue analogues. Indicated are the sites for the atoms involved. The cell parameter (cell edge size) corresponds to the M–N≡C–Fe–C≡N–M chain length.

bonded interactions. The crystal structures of the samples studied were refined in that structural model with excellent figures of merit. Experimental and fitted XRD patterns are available at stacks.iop.org/JPhysCM/18/11243. The resulting structural data (atomic positions, interatomic distances and bond angles, occupation and temperature factors, and fitting figures of merit) have been deposited at ICSD crystal data base (Fachinformationszentrum Karlsruhe (FIZ); email: crysdata@fiz-karlsruhe.de) with the following ICSD file numbers: 416993: $Co_3[Fe(CN)_6]_2{\cdot}15H_2O$; 416994: $Mn_3[Fe(CN)_6]_2{\cdot}14H_2O$; 416995: $Cu_3[Fe(CN)_6]_2{\cdot}10H_2O$; 416997: $Ni_3[Fe(CN)_6]_2{\cdot}16H_2O$. Figure 2 shows the unit cell for this series of materials indicating the position of both coordinated and zeolitic water molecules. The 3D structure is formed by orthogonal linear chains $\cdots$M–N≡C–Fe–C≡N–M$\cdots$. The estimated hydration degrees, from the refined water oxygen atom occupation factors, indicated in the given unit formula, were similar to those calculated from the TG curves (figure 1, inset (a); table 1). These materials are highly hydrated solids, with up to 16 water molecules per unit formula. In the unit formula only six water molecules remain coordinated to the metal (M); the remaining ones have zeolitic nature and are found forming a small cluster within the larger pores (figure 2).

Both coordinated and zeolitic waters can be removed through a moderate heating, usually below 100 °C (figure 1, inset (a)). In the IR spectra of the evolved gases (not shown) no absorption bands due to water vapour were detected above 100 °C except for Ni, which required up to 120 °C for a complete dehydration at normal pressure. Ni(2+) is the metal with the highest polarizing power within the metal ions considered [19], and because of this it is the one for which the strongest bond with the coordinated waters is observed. Compared to zeolites, for instance, porous cyanometallates require relatively low temperature of heating to obtain anhydrous samples because these latter are usually free of strong charge centres like alkali ions [20]. The resulting anhydrous materials then remain stable up to above 150 °C where their decomposition is detected through the evolution of C_2N_2 and ferrocyanide formation. This is an already-documented process [21]. For copper the decomposition process begins at relatively low temperature, about 135 °C ((figure 1, inset (a)). Copper ferricyanide is the most unstable member for the family of transition metal ferricyanides. The copper complex also corresponds to the smaller cell parameter (table 1), indicating that the copper and iron atoms are involved in

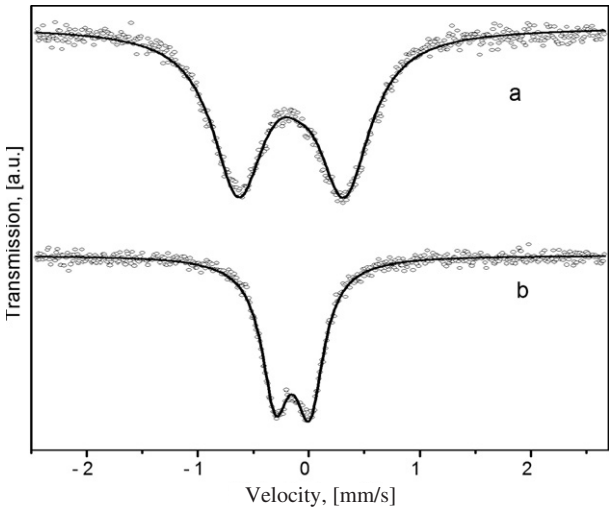

Figure 3. Mössbauer spectra at room temperature of Mn(2+) hexacyanoferrate (III): (a) anhydrous sample; (b) hydrated sample (saturated in water).

a particularly strong interaction through the CN bridges. This strong interaction was attributed to the ability of the CN group to donate an electron from its 5σ orbital, which has certain antibonding character, and to the copper (2+) ion capability to accept that charge in its 3d hole to attain an electronic configuration close to $3d^{10}$. An evidence of that interaction is the low hydration degree found for copper (table 1), attributed to a reduced effective positive charge on the copper ion. Probably the low thermal stability observed for copper ferricyanide is related to such unique bonding features for the copper atom.

On the removal of water a progressive cell contraction was observed, which amounts to 4% of the cell volume reduction (table 1), as estimated from XRD powder patterns recorded in vacuum for annealed samples (figure 1, inset (b)). Once all the crystal water has been removed no variation in the cell parameter is observed. This is a reversible effect. On sample rehydration the cell edge size is restored. Such cell parameter variation with water removal and adsorption reveals a change in the metal–metal interaction through the CN bridges (discussed below). The cell edge corresponds to the M–N≡C–Fe–C≡N–M chain length. The dehydration and rehydration processes take place preserving the cell symmetry as cubic, indicating that the metal–metal interaction path (M–N≡C–Fe–C≡N–M) remains linear.

3.2. Mössbauer spectra

Figure 3 shows typical Mössbauer spectra for the ferricyanides considered in their hydrated and anhydrous forms. In table 2 the estimated Mössbauer parameters for all the samples studied with different adsorbed species are collected. Without exception, water removal leads to an increase in the doublet quadrupole splitting (Δ) value. This is a reversible process. When water vapour is adsorbed on an anhydrous sample, the quadrupole splitting value decreases. The pore filling with other guest species has an analogue effect but is less pronounced. For N_2 the critical temperature is very low, −147 °C [22], to allow nitrogen molecule condensation within the pores. For CO_2 the critical temperature is 31 °C [22], and the adsorption process takes place in practically supercritical conditions for this adsorbate. For CO_2 the pore filling must also be low. From these facts the N_2 and CO_2 adsorption at room temperature has a

Table 2. Mössbauer parameters at room temperature of the microporous molecular magnets studied with different adsorbed (guest) species. (Note that the estimated errors in δ, Δ and Γ remain below 0.01 mm s^{-1}. The values of δ are reported relative to sodium nitroprusside.)

Assembling metal	Sample state or adsorbed (guest) species	δ (mm s^{-1})	Δ (mm s^{-1})	Γ (mm s^{-1})
Mn	Without guest species	0.100	0.944	0.60
	N_2	0.101	0.931	0.59
	CO_2	0.102	0.923	0.59
	Ethanol	0.105	0.870	0.58
	Methanol	0.106	0.684	0.56
	Water vapour	0.111	0.273	0.29
Co	Without guest species	0.099	0.974	0.56
	N_2	0.098	0.957	0.56
	Ethanol	0.105	0.870	0.58
	Methanol	0.106	0.684	0.56
	Water vapour	0.118	0.427	0.32
Ni	Without guest species	0.104	1.023	0.57
	N_2	0.103	0.989	0.56
	Ethanol	0.106	0.934	0.51
	Methanol	0.107	0.607	0.49
	Water vapour	0.112	0.497	0.34
Cu	Without guest species	0.097	0.908	0.47
	N_2	0.098	0.893	0.46
	CO_2	0.098	0.881	0.46
	Ethanol	0.101	0.672	0.41
	Methanol	0.102	0.635	0.42
	Water vapour	0.105	0.543	0.31

minor effect on the Mössbauer parameters of the samples studied. A different behaviour was observed for vapours of water, ethanol and methanol, probably because these three adsorbates can be condensed with the pores facilitating the guest–host interactions. Between the estimated values for Δ and δ certain negative correlation was observed (table 2). An increase in Δ is related to a decrease in δ.

The Mössbauer spectra of hexacyanoferrates (III) are quadrupole doublets, not only due to the unpaired electron in the iron t_{2g} orbitals but also from a local distortion around the iron atom induced by the metal ion at the pore surface. This last contribution to the value of Δ becomes evident when spectra of the different compounds (in their hydrated form) are compared. The larger Δ values correspond to metal ions of stronger interaction with their coordination environment (Cu, Ni) (table 2). The metal centres (M and Fe) remain strongly linked through the CN bridges, and any local distortion at the pore surface is partially transmitted to the iron atom coordination sphere and sensed through the value of Δ. The observed negative correlation between the isomer shift and quadrupole splitting values also results from an induced effect. The interaction at the N end of the CN group modulates the π^* back-donation at the C end and this leads to a change in the 3d electron population at the iron atom and to its shielding effect on the s electron density at the iron nucleus. An increase in the 3d electron density on the iron atom leads to a decrease in the value of δ, and, similarly, a 3d charge subtraction from the iron atom is sensed as an increase of δ. As will be discussed below, such modulation in the π^* back-donation at the iron atom determines the studied effect of the adsorbed species on the material magnetic properties. In the absence of guest species within the pore the metal ion at the pore surface has its coordination sphere unsaturated; on average it remains linked to only

four N ends of the CN groups. When the pore is occupied by polar guest molecules (e.g. water, ethanol, methanol) they behave as ligands for the metal, contributing to saturate its coordination sphere. This leads to a reduction in the local distortion around the metal centres, observed as a decrease for the value of Δ. The surface interaction with the guest molecules also reduces the metal charge subtraction from the CN group at the N end, weakening the π^* back-bonding at the iron atom. This results in an increase for the value of δ (table 2). For guest molecules with low ability to interact with the metal, for instance N_2 and CO_2 with only quadrupole moment, and also with a low population within the pores, the values obtained for Δ are similar to those found for unoccupied pores (table 2). Within the guest species evaluated, the smallest Δ values were found when the pores were completely filled by water molecules. Water is a small and polar molecule which participates in a strong interaction with the metal, particularly the first adsorbed molecules sited in the metal coordination environment. However, according to the XRD data (figure 1, inset (b)), the adsorption or removal of zeolitic waters also has a certain effect on the metal–metal interatomic distance, and in their interaction. Such an effect is related to the formation of hydrogen bridges between coordinated and zeolitic waters. For the guest molecules used, the strength of the host–guest interaction can be ordered according to the observed variation of Δ: $N_2 \sim CO_2 <$ ethanol $<$ methanol $<$ water (table 2). Therefore, the magnetic measurements were limited to the material with and without adsorbed water.

The cubic structure for the materials studied corresponds to a random distribution for the vacant octahedral block, $[Fe(CN)_6]$. In such a structure different local configurations for the metal coordination environment are expected, $M(NC)_{6-x}(H_2O)_x$, with $x = 2$ as average value. The Mössbauer spectra for this family of materials appear as a doublet of broad lines, suggesting the existence of a slightly different local environment for the metal (M) at pore surface. In the anhydrous material different local configurations could also be found, with $M(NC)_4$ as the most probable and average ligand configuration, but not the only one. The line broadening is particularly notable for the anhydrous state of a given sample (figure 3) where the different coordination geometries for the metal linked at the N end produce a wide variation in the value of Δ. From a structural point of view, the $M(NC)_4$ (pseudo-tetrahedral) and $M(NC)_4(H_2O)_2$ (pseudo-octahedral) coordination for the anhydrous and hydrated samples, respectively, only represent the average values, and not two well-defined coordination geometries [4]. The existence of a pure tetrahedral coordination, $M(NC)_4$, is not possible within the cubic structure of PB analogues. For instance, zinc ferricyanide is a dimorphic material: cubic ($Fm\bar{3}m$) and rhombohedral ($R\bar{3}c$). The cubic phase is an hydrate where the zinc atom has a mixed coordination sphere, $Zn(NC)_4(H_2O)_2$. When this cubic phase is heated and the crystal water evolves, a structural transformation takes place, with formation of the rhombohedral phase in which the Zn atom has a pure tetrahedral coordination, $Zn(NC)_4$ [21]. In the rhombohedral structure the Zn–N≡C–Fe–C≡N–Zn chain is nonlinear. The rhombohedral modification is a hydrophobic material because the zinc has saturated its coordination sphere. The Mössbauer spectrum for the $R\bar{3}c$ phase of zinc ferricyanide is an unresolved quadrupole doublet ($\Delta = 0.18$ mm s^{-1}), indicating that both iron and zinc atoms have highly symmetric coordination environments.

3.3. Magnetic data

Figures 4 and 5 show representative zero-field-cooled magnetization (M_{ZFC}) curves for Mn(2+) and Cu(2+) hexacyanoferrates (III) with and without adsorbed water for an applied field (H) of 0.4 kA m^{-1} (5 Oe). Below 20 K the observed M_{ZFC} versus T dependences are typical of magnetic materials. An analogous behaviour was observed for Co(2+) and Ni(2+) ferricyanides (see supplementary data available at stacks.iop.org/JPhysCM/18/11243). From the minimum for the derivative dM_{ZFC}/dT curve (figures 4 and 5, insets) the Curie temperature

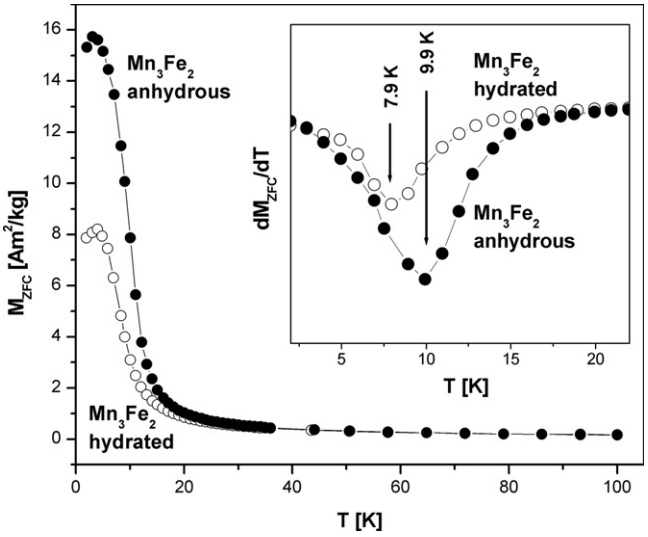

Figure 4. Zero-field-cooled magnetization curve for Mn(2+) hexacyanoferrate (III) (Mn_3Fe_2), at an applied field of 5 Oe, in anhydrous (in vacuum) and hydrated states. Inset: derivative curves used to estimate the T_C value.

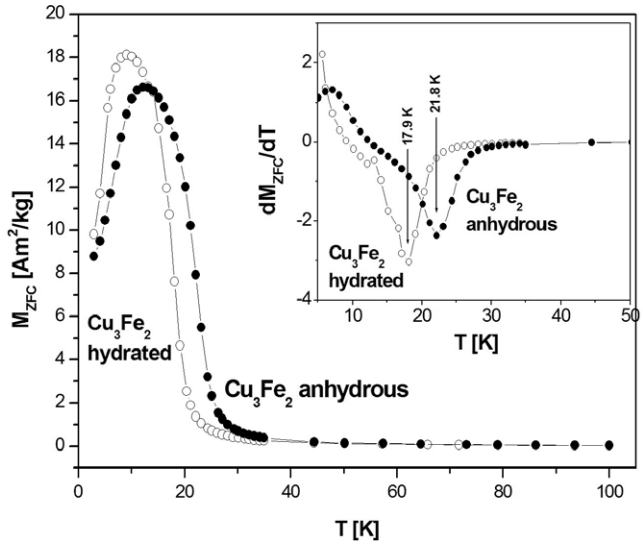

Figure 5. Zero-field-cooled magnetization curve for Cu(2+) hexacyanoferrate (III) (Cu_3Fe_2), at an applied field of 5 Oe, in anhydrous (in vacuum) and hydrated states. Inset: derivative curves used to estimate the T_C value.

(T_C) was estimated. The higher values for T_C are obtained for the anhydrous samples (table 3). Figure 6 shows the reciprocal mass susceptibility ($1/\chi_p$) versus temperature (T) curves for these two compounds in their hydrated and anhydrous forms. The Curie (C) and Curie–Weiss (θ_{CW}) constants were estimated through a linear fitting of these last curves according to the Curie–Weiss law, $1/\chi_p = (T - \theta_{CW})/C$. The values obtained for C and θ_{CW} are collected in table 3. The larger values for θ_{CW} also correspond to the anhydrous phase.

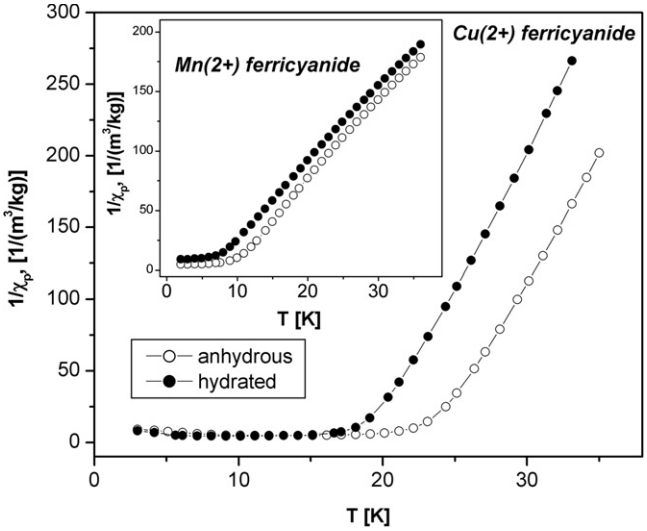

Figure 6. Reciprocal mass susceptibility ($1/\chi_p$) versus temperature (T) curves used to estimate the Curie (C) and Curie–Weiss (θ_{CW}) constants for Mn(2+) and Cu(2+) ferricyanides in their hydrated and anhydrous states.

Table 3. Magnetic parameters for the materials studied as anhydrous (without guest species) and hydrated (with water vapour adsorbed) samples.

Sample	T_C (K)	θ_{CW} (K)	Abs (J) (cm^{-1})
Mn_3Fe_2 without guest species	9.9	7.58	2.11
Mn_3Fe_2 with water vapour adsorbed	7.9	5.20	1.68
Co_3Fe_2 activated	14.4	13.98	4.04
Co_3Fe_2 with water vapour adsorbed	13.5	11.77	3.76
Ni_3Fe_2 without guest species	24.9	27.13	8.83
Ni_3Fe_2 with water vapour adsorbed	18.9	22.58	6.70
Cu_3Fe_2 without guest species	21.8	23.99	11.24
Cu_3Fe_2 with water vapour adsorbed	17.9	19.65	9.23

For the samples studied two types of magnetic behaviour are expected. For Mn and Co the magnetic ordering must be of ferrimagnetic type, which results from combined effects of unpaired electrons sited in orthogonal orbitals, t_{2g} from Fe and e_g from Mn and Co (ferromagnetic contribution), and those sited in non-orthogonal ones, t_{2g} (Fe) and t_{2g} (Mn, Co) (antiferromagnetic contribution). A certain antiferromagnetic contribution is also expected from interaction between second-nearest neighbours, the M atoms, but it is very weak because these atoms are separated by more than 10 Å. For Ni and Cu the magnetic ordering must be of ferromagnetic type because it proceeds from the interaction of electrons in orthogonal orbitals, t_{2g} on the iron atom and e_g on the outer metal ion (Ni, Cu). This supposes a non-significant antiferromagnetic contribution from second neighbours. Such magnetic behaviours are supported by the positive value obtained for the Curie–Weiss (θ_{CW}) constant (table 3).

The observed decrease in the value of T_C and θ_{CW} on the adsorption of water reveals a weakening of the metal–metal interaction related to the formation of a coordination bond between water molecules and the metal ion at the pore surface. This experimental evidence regarding a change in the material electronic structure due to the guest–host interaction agrees

with the results from the XRD and Mössbauer data discussed above. The lower T_C and θ_{CW} values correspond to the hydrated phase where the metal centres are more distant, i.e., the larger cell parameter. The Mössbauer results are also conclusive. The isomer shift value (δ) senses the effective 3d electron density on the iron atom, which has a minimum for the absence of a guest species within the pores. The observed variation in T_C and θ_{CW} cannot be attributed to a deviation of the Fe–C≡N–M–N≡C–Fe chain from linearity because on the sample dehydration and rehydration the cell symmetry is preserved.

From the obtained value for T_C the variation in the exchange coupling constant (J) between the metal centres, neglecting the contribution from second neighbours, can be estimated according to [23]

$$T_C = \frac{2}{k} y\sqrt{y}|J_{FeM}|\sqrt{S_{Fe}(S_{Fe}+1)S_M(S_M+1)},$$

where k is the Boltzmann constant, y is the metal ratio in the formula unit, $S_{Fe}(=1/2)$, and S_M is the net spin due to the unpaired electrons in the metal. The calculated J values appear in table 3. Without exception the interaction of the guest molecule, in this case water, with the metal at the pore surface induces a weakening of the π^* back-donation at the iron atom and this results in a weaker super-exchange interaction between the metal centres, i.e., a smaller J value.

The larger value for J was observed for copper ferricyanide, which was attributed to the particularly strong interaction between the copper ion and the CN groups discussed above. The smaller isomer shift values within the series of compounds studied (table 2) also corresponds to copper. The copper atom interaction with the CN ligand at the N end induces a large charge delocalization from the iron atom towards the ligands.

The variation of the magnetic properties related to the dehydration and rehydration processes has been reported for other molecular materials [9, 10]. However, the effect discussed above is independent of the guest molecule used. The properties of the guest species determine the intensity of the effect but not its nature. In this sense the materials studied appear as appropriate model systems to shed light on the modulation of the electronic structure in porous material through adsorbed species.

4. Conclusions

The interaction of the guest molecules with the metal at the pore surface of microporous molecular magnets based on PB analogues induces a weakening of the π^* back-donation at the iron atom and this leads to a reduction in the charge overlapping between the metal centres. XRD and Mössbauer data are conclusive in that sense. Such an effect is responsible for the variation in the values of T_C, θ_{CW} and J observed in the materials studied upon water vapour adsorption and desorption. This effect is inherent to the nature of the material and not to a particular guest molecule, as revealed by Mössbauer spectroscopy. The stronger the metal–adsorbate interaction, the larger is the expected variation in the electronic structure of the host framework and, consequently, in the magnetic properties. The variation in the exchange constant (J) depends on the transition metal involved, ranging from 7 (Co) to 24% (Ni). This is a remarkable effect on the super-exchange interaction, at least through an adsorption process. The results obtained illustrate that in porous PB analogue-based molecular magnets the magnetic properties can be properly modulated by the adsorbed species. The observed variation in the magnetic properties of PB analogues on water adsorption and desorption cannot be attributed to a change in the coordination geometries, from octahedral to tetrahedral, for the metal ion at the pore surface on the removal of water. The existence of a tetrahedral coordination is not possible in the cubic structure of PB analogues.

Acknowledgments

The authors thank the LNLS synchrotron radiation facility (Campinas, Brazil) for XRD data acquisition. RMG acknowledges the support provided by the CLAF-ICTP program for his PhD studies. The partial support provided by FAPESP and CNPq (Brazilian agencies) is also acknowledged.

References

[1] Ferlay S, Mallah T, Ouahes R, Veillet P and Verdaguer M 1995 *Nature* **378** 701
[2] Holmes S M and Girolami G S 1999 *J. Am. Chem. Soc.* **121** 5593
[3] Sato O, Iyoda T, Fujishima A and Hashimoto K 1996 *Science* **272** 704
[4] Ohkoshi S, Arai K, Sato Y and Hashimoto K 2004 *Nat. Mater.* **3** 857
[5] Buschmann W E, Ensling J, Gütlich P and Miller J S 1999 *Chem. Eur. J.* **5** 3019
[6] Kaye S S and Long J R 2005 *J. Am. Chem. Soc.* **127** 6506
[7] Hartman M R, Peterson V K, Liu Y, Kaye S S and Long J R 2006 *Mater. Chem.* **18** 3221
[8] Chapman K W, Chupas P J and Kepert C J 2006 *J. Am. Chem. Soc.* **128** 7009
[9] Larionova J, Chavan S A, Yakhmi J V, Froystein A G, Sletten J, Sourisseau C and Khan O 1997 *Inorg. Chem.* **36** 6374
[10] Kurmoo M, Kumagai H, Hughes S M and Kepert C J 2003 *Inorg. Chem.* **42** 6709
[11] Brauer G 1965 *Handbook of Preparative Inorganic Chemistry* 2nd edn, vol 2 (New York: Academic) p 1373
[12] Fernandez-Bertran J and Reguera E 1996 *Solid State Ion.* **93** 139
[13] Boultif A and Louer D 1991 *J. Appl. Crystallogr.* **24** 987
[14] Rodríguez-Carbajal J 1998 *The FullProf Program* Institute Louis Brilloin, Saclay, France
[15] Larson A C and Dreele R B V 2000 *GSAS: General Structure Analysis System*
[16] Ferreira F F, Granado E, Carvalho W Jr, Kycia S W, Bruno D and Droppa R Jr 2006 *J. Synchrotron Radiat.* **13** 46
[17] Nakamoto K 1986 *Infrared and Raman Spectra of Inorganic and Coordination Compounds* (New York: Wiley) p 484
[18] Ludi A and Gudel A 1973 *Struct. Bonding* **14** 1
[19] Zhang Y 1992 *Inorg. Chem.* **21** 3889
[20] Balmaseda J, Reguera E, Gomez A, Roque J, Vazquez C and Autie M 2003 *J. Phys. Chem.* B **107** 11360
[21] Martinez-Garcia R, Kobel M and Reguera E 2006 *J. Phys. Chem.* B **110** 7296
[22] Medard L (ed) 2002 *Gas Encyclopaedia* 3rd edn (The Netherlands: Elsevier)
[23] Ferlay S, Mallah T, Ouahes R, Veillet P and Verdaguer M 1999 *Inorg. Chem.* **38** 229